Acoustics 2008
Geelong, Victoria, Australia 24 to 26 November 2008

Acoustics and Sustainability:

How should acoustics adapt to meet future demands?

Preliminary characterisation and analysis of snapping shrimp noise from the Nornalup-Walpole Estuary

Legg, M.W. (1)(2)*, Killeen, D.S. (1)(2) and Duncan, A.J. (2)

(1) MOD, Defence Science and Technology Organisation, HMAS Stirling, Western Australia
(2) CMST, Curtin University of Technology, Bentley, Western Australia

ABSTRACT

During September 2006, an exploratory underwater acoustic recording was made in the Nornalup-Walpole Estuary located 350 km south of Perth, Western Australia. Immediately obvious in the recording was a sustained crackling sound, characteristic of snapping shrimp. The presence of snapping shrimp in the estuary was unexpected, since the salinity is generally quite low, and snapping shrimp were not mentioned in biological literature surveyed prior to the recording. Individual impulses showed precursor and bubble characteristics, and spectral and statistical properties of the impulsive noise were consistent with the source being the snapping shrimp.

INTRODUCTION

The Nornalup-Walpole Estuary is situated on the southern coast of Western Australia, approximately 350 km south of Perth. Fed by the mostly freshwater Walpole River, the Walpole Inlet joins the larger Nornalup Inlet before entering the southern ocean between East Point and Bellanger Beach. Figure 1 shows a summary chart of the estuary system (courtesy of the Department of Planning and Infrastructure). Features of the system are the Walpole, Frankland and Deep Rivers, the Walpole and Nornalup Inlets, and a permanently open entrance channel near Skippy Rock.

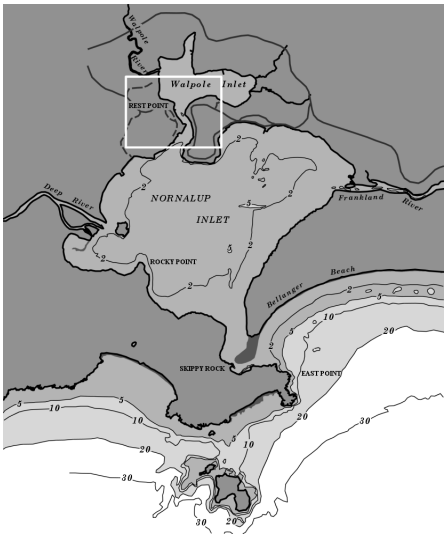

Figure 1. Summary of DPI chart Nornalup Inlet WA 1046 (used with permission).

A large variety of fauna exist in the inlets, among the recreationally important fish are the Black bream (*Acanthopagrus butcheri*), King George whiting (*Sillaginodes punctata*) and the Herring (*Arripis georgianus*). Among the Crustacea found in the Walpole Inlet are members of the orders *Cirripedia, Mysidacea, Amphipoda* and *Decapoda*. Of the Decapoda only small numbers of *Halicarcinus ovatus* (oval spider crab) and *Palaemonetes australis* (a type of carid shrimp) were reported by Hodgkin and Clark (1999). No members of the *Alpheidae* (snapping shrimp) family were reported.

Temperature and salinity levels in the inlets vary seasonally. Monthly mean surface temperatures for most of the year 1990 were reported by Neira and Potter (1994). Temperatures in the Walpole Inlet varied between a maximum of 24.1 °C in March, and a minimum of 10.7 °C in July. Salinity variations over a similar period were between 35.7 [ppt] in January and 2.0 [ppt] in July. Salinity units omitted in (Neira & Potter 1994) were assumed to be parts-per-thousand (ppt) consistent with Hodgkin and Clark (1999). Marine sediment in the Walpole Inlet is fine organic mud (Hodgkin & Clarke 1999).

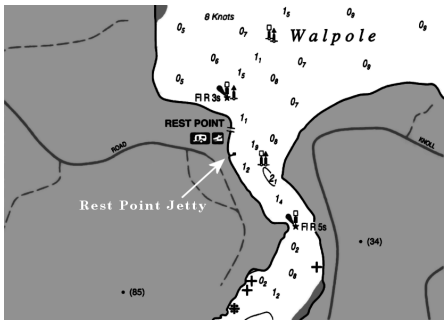

Figure 2. The Rest Point jetty extended approximately 25 m over the water into a channel from the Walpole Inlet.

MEASUREMENT METHOD

Exploratory underwater acoustic measurements were conducted in September 2006 from the Rest Point jetty located at 34°59.3′ S, 116°43.3′ E. The jetty extended approximately 25 m over the water near a channel that joins the Walpole and Nornalup Inlets, as shown in Figure 2.

Acoustic recordings were made using an HTI-96-MIN preamplified hydrophone (nominal sensitivity -164 dB re 1V per µPa) connected to the line input of a portable digital audio tape (DAT) recorder. A -20 dB re 1V band limited (20 kHz) white noise signal from a Neutrik MR1 audio signal generator was used to calibrate the DAT recorder.

The hydrophone was secured from the south eastern corner of the jetty at a depth of 0.5 m, and recording commenced using a sample rate of 48 kHz. Higher sample rate equipment was not used due to the exploratory nature of the recording, and equipment portability considerations. A single continuous recording was made over a period of 42 minutes, during which a number of scraping sounds could be heard. The scraping sounds were thought to be caused by stingrays contacting the hydrophone cable, although this could not be confirmed visually. During the recording several people visited the jetty, and some of the visitors commenced fishing. Various transient signals were caused by this activity, including the sound of a fish (*Arripis georgianus*) being caught.

Upon completion of the recording, the water depth was measured by further lowering the hydrophone until it lightly touched the estuary floor. The water line was marked and the depth measured as 1.2 m. Due to the exploratory nature of the acoustic recordings, physical properties of the water, such as temperature and salinity, were not measured at the time of recording.

RESULTS

A 300 second section of raw pressure amplitudes were plotted as a time-series in Figure 3. The time-series contained many high pressure impulses interspersed randomly throughout a relatively low pressure background. The origin of the high pressure impulses was thought to be the snapping shrimp, a common source of such impulsive noise observed in warm shallow seas (Potter & Chitre 1999), and possibly in some colder waters (Finfer et al. 2007). The following analysis was conducted to investigate the characteristics of the high pressure impulses, to see if they exhibit the same characteristics as the snaps produced by snapping shrimp.

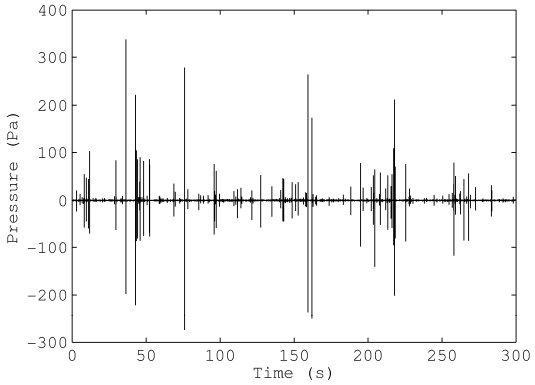

Figure 3. A section of the pressure time-series measured at the Rest Point Jetty site. High pressure impulses characteristic of snapping shrimp are clearly visible.

Snap acoustic signature

Acoustic impulses produced by shrimp snap are caused by a cavitation bubble (Versluis et al. 2000). The acoustic signature of shrimp snaps are well defined, containing a precursor, a bubble development and bubble collapse region, and a main peak caused by bubble rebound. These regions were all identified in snaps from the Walpole Inlet, and shown for a representative snap in Figure 4. Due to the limited bandwidth the main peak is broader than reported by Cato & Bell (1992) and Au & Banks (1998). Following the main peak was a region of after effects, which contained another well defined peak; potentially a bottom reflected replica of the type reported by Chitre, Koay and Potter (2003).

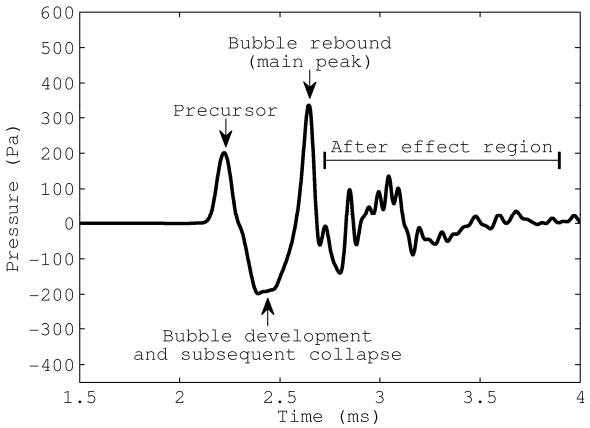

Figure 4. The acoustic signature of an individual impulse showing characteristic features of a shrimp snap.

Spectral analysis

Several of the higher amplitude impulses were selected for spectral analysis, one of which was shown in Figure 4. For each impulse, 512 sample points were chosen so that the peak pressure of the impulse occurred at sample number 128. The mean pressure was computed using the first 80 samples (1 ms prior to peak pressure), then subtracted from each of the 512 samples to give a set of zero-offset time-series points. Time delays between the start of the precursor and the main peak were compared with similar results reported from tank measurements (Au & Banks 1998). The time delays were measured from the first sample that exceeded an empirically determined threshold of 2.5 Pa, to the positive-going zero-pressure crossing of the main peak. Delays shown in Table 1 ranged from 0.46 ms to 0.58 ms, which were significantly longer than the approximately 0.29 ms delay reported by Au and Banks (1998).

Table 1. Time delays between precursor and main peak

Snap #	*Delay (ms)*	*PSD peak (kHz)*	*Null separation (kHz)*	*Null time separation (ms)*
1	0.46	2.25	2.2	0.46
2	0.40	2.25	1.9	0.51
3	0.58	1.88	1.6	0.64
4	0.56	1.88	1.6	0.62
5	0.50	1.88	1.8	0.57
6	0.50	1.88	2.1	0.49
	±0.02		±0.1	±0.03

One-sided power spectral densities (PSD) were computed using a single periodogram without shading. An example (using the snap from Figure 4) is shown in Figure 5. When using the entire 512 sample section of time-series to estimate the spectral density (grey line), around 8 ms of reverberation following the snap was included in the estimate. These spec-

tral densities contained structure associated with the impulse response of the propagation channel as well as from the snaps themselves.

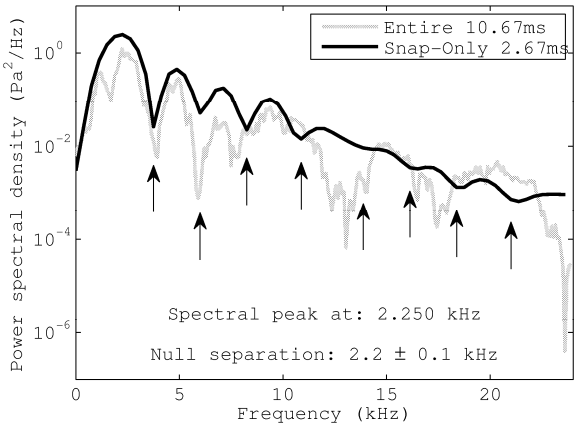

Figure 5. Power spectral density curves for a single shrimp snap. Nulls in the shorter (snap-only) density curve are indicated using arrows.

To reveal more detail about the snaps, a short region was chosen from each snap (up to the first negative-going zero-pressure crossing after peak pressure) along with some of the preceding background noise and the power spectral density re-computed. This "snap-only" spectral density (a black line for the example shown in Figure 5) used 128 samples (2.67 ms), rather than the entire 512 samples, and contained much less reverberation. All spectral densities had a primary peak near 2 kHz (see Table 1) and spectral ripple as reported by Au and Banks (1998). The spectral ripple was due to interaction between the precursor pulse and the slow rise in pressure as the bubble starts to collapse.

The spacing between consecutive spectral nulls was determined by computing the difference between consecutive gradients of the logarithm of the shorter spectrum. All positive-valued maxima of this function were considered nulls in the original spectra, such as those shown by arrows in Figure 5. A linear least-squares fit to the frequencies of these nulls was performed. The gradient of the least squares fit was used as an estimate of the underlying null separation. For the snap shown in Figure 5 the null separation was 2.2±0.1 kHz.

According to Au and Banks (1998) the null separation should be inversely-proportional to the time delay between the start of the precursor and the start of the main snap. This was indeed the case for snaps 1 and 6 detailed in Table 1. Snaps 2 through 5 differ by respectively 15, 2, 4, and 4 percent.

Time-frequency analysis

An effort was made to compute the time evolution of the spectral characteristics of a single snap. The same representative snap shown in Figure 4 was used. Successive, un-shaded power spectral densities were computed, each using 64 samples. The start of each successive spectral density was offset by 16 samples (0.33 ms), allowing for 29 spectral densities within the entire 512 sample section. The spectral densities were plotted as a function of elapsed time using a waterfall plot in Figure 6. The first three spectra in the time evolution showed that the background noise level (preceding the snap) was on average six to eight orders of magnitude lower in power spectral density than the snap itself.

The fourth spectrum (greyed) showed the start of the snap pulse (dominated by the precursor) and contained most of its energy in the lower frequencies, as reported by Au and Banks (1998). The fifth spectrum, (also grey) displayed a spectral peak near 2 kHz and spectral ripple as described in the previous section. The spectra occurring after the snap event showed a relatively slow decay due to the highly reverberant environment.

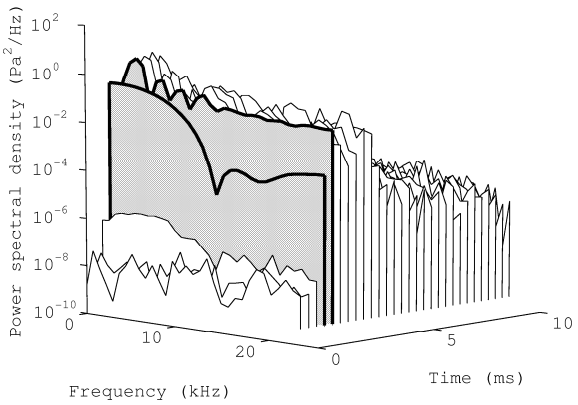

Figure 6. Waterfall plot showing the time evolution of spectral characteristics of an impulsive shrimp snap. The two grey spectra contain important information about the snap.

Amplitude statistics

The empirical probability density of the instantaneous pressure amplitudes was computed using a scaled and logarithmically smoothed histogram estimator. All of the available time-series pressure amplitudes were counted into 1800 equally sized bins and appropriately scaled, giving linearly spaced empirical probability density estimates.

To improve the probability density estimates towards the tails of the distribution, where count numbers were expected to be low, the linear results were logarithmically smoothed. Assuming a near zero mean value of the pressure amplitudes, the smoothing algorithm sectioned the pressure space into base 2 logarithmically sized windows. The size of the windows increased with both increasing positive and increasing negative pressure. The final probability density was computed as the mean value of all empirical probability densities within each window.

Figure 7 was used to show the empirical probability density function (dot markers) plotted as a function of pressure using logarithmic axes. Also shown were Gaussian (solid line) and Gaussian-Gaussian mixture (dashed line) models. At small pressure values the empirical density function was approximately Gaussian, but at higher pressures the empirical results departed markedly from Gaussian, displaying *heavy tails* characteristic of impulsive noise.

Three distinct regions were identified in the empirical density function: a small pressure or *head* region, where the results were approximately Gaussian; a medium pressure or *shoulder* region, where the empirical results moved smoothly away from and above the Gaussian model and; a high pressure or *tail* region (beyond ±100 Pa) where a second, high variance, Gaussian enabled the mixture model to rejoin with the empirical results.

The mixture model (dashed line) showed in Figure 7 used two Gaussian distributions, one to model the background noise and another, with much higher variance, to model the impulsive noise as described by Aazhang and Poor (1987). Such models can be conveniently described using the ratio of the Gaussian variances. Common ratio values for impulsive noise are 10 to 100, however values as high as 10^4 could be considered reasonable (Vastola 1984). The mixture model shown in Figure 7 used a variance of 0.15 for the background

Gaussian and 9.5×10^3 for the impulsive Gaussian, giving a ratio of 6.18×10^4.

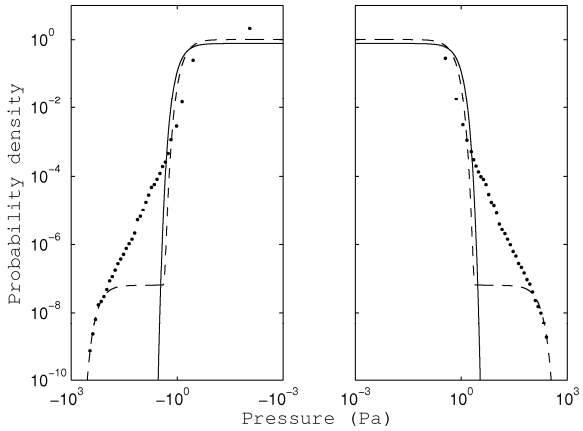

Figure 7. Empirical probability density function (dot markers) of instantaneous pressure amplitudes shown using log-log scales. Also shown are Gaussian (solid line) and Gaussian-Gaussian mixture (dashed line) models.

The validity of amplitude statistics derived from low sample rate (48 kHz) data may be questionable, given the extremely high bandwidth of individual shrimp snaps. However, ensemble shrimp noise from other locations sampled at 192 kHz showed relatively minor changes in the shape of the amplitude statistics when down-sampled to 48 kHz. The main effect of down-sampling was to reduce the minimum and maximum pressure excursions.

DISCUSSION

Acoustic time-series measured from the Rest Point jetty were visually and aurally similar to shallow-ocean acoustic time-series that contain impulsive noise produced by snapping shrimp. Closer examination of individual impulses revealed acoustic signatures of the precursor, bubble development and bubble collapse expected from snapping shrimp. Due to the mechanism producing the sound, the precursor and main peak pressures were expected to always be positive. Inspection of the higher pressure snaps showed this to be the case, further supporting the snapping shrimp source hypothesis. Time delays between the precursor and main snap did not agree with similar results from tank measurements conducted by Au and Banks (1998), although spectral analysis showed a spectral peak near 2 kHz and spectral ripple with the expected null separations. Possible reasons for the difference were thought to be the type of shrimp (and hence the size of the claw), and the propagating environment. It was not known if the precursor characteristic of the shrimp snap was unique, which would allow a definite conclusion that the source was snapping shrimp. No sample specimen of a snapping shrimp was found, so the possibility of other sources producing the impulses was not discounted entirely. In light of the acoustic evidence the snapping shrimp was considered the most likely source of the observed acoustic impulses.

Spectral analysis showed that the background noise level (preceding the snap) was on average six to eight orders of magnitude lower in power spectral density than the snap itself. Estimation of the power spectral density was conducted using a single periodogram because the number of samples covering the snap interval was low. Shading was not used because of the very short time duration of the impulse and for consistency with the time evolution spectra. A first order probability density function of the instantaneous pressure amplitudes was computed from the entire time-series. The probability density function deviated from a Gaussian fit, with heavy tails characteristic of impulsive noise. A Gaussian-Gaussian mixture fit was able to better model the extreme tails of the distribution but was not able to describe the distribution over the entire range of pressures.

Higher sample rate recordings would allow smoother estimates of the power spectral density, and improve the identification of precursor, main peak and possibly a bottom reflected replica from the acoustic time-series. For these reasons a high sample rate recording was planned for future research.

CONCLUSION

An exploratory underwater acoustic recording was conducted in the Nornalup-Walpole Estuary during September 2006. The acoustic recordings contained numerous high pressure impulses. The impulses were on average six to eight orders of magnitude higher in spectral density than the background noise, and the ratio of variances of a Gaussian-Gaussian mixture model of pressure amplitudes was 6.18×10^4. Investigation of the acoustic pressure time-series and spectral analyses showed that the origin of impulses was most likely the snapping shrimp (members of the *Alpheidae* family).

REFERENCES

Aazhang, B. & Poor, H.V. 1987, 'Performance of DS/SSMA communications in impulsive channels – Part 1: linear correlation receivers', *IEEE Trans. Commun.*, vol. COM-35, no. 11, pp. 1179-1188.

Au, W.L.L. & Banks, K. 1998, 'The acoustics of the snapping shrimp *Synalpheus parneomeris* in Kaneohe Bay', *J. Acoust. Soc. Am.,* vol. 103, no. 1, pp. 41-47.

Chitre, M. Koay, T.B. & Potter J.R. 2003,'Origins of directionality in snapping shrimp sounds and its potential applications', *OCEANS 2003 Marine Technology and Ocean Science Conference (MTS/IEEE)*, San Diego USA, pp. 889-896.

Cato, D.H. & Bell, M.J. 1992, 'Ultrasonic ambient noise in Australian shallow waters at frequencies up to 200 kHz', *Materials Research Laboratory Technical Report MRL-TR-91-23*, Melbourne, Australia.

Finfer, D.C. White, P.R. Leighton, T.G. Hadley, M. & Harland, E. J. 2007, 'On clicking sounds in UK waters and a preliminary study of their possible biological origin', *Fourth International Conference on Bio-Acoustics*, Loughborough, pp. 209-216.

Hodgkin, E.P. & Clark, R. 1999, 'Nornalup and Walpole Inlets and the estuaries of the Deep and Frankland Rivers', Estuarine Studies Series - No 2, Environmental Protection Authority, Perth.

Neira, F.J. & Potter, I.C. 1994, 'The larval fish assemblage of the Nornalup-Walpole Estuary, a permanently open estuary on the southern coast of Western Australia', *Aust. J. Mar. Freshwater Res.*, vol. 45, no. 7, pp. 1193-1207.

Potter, J.R. & Chitre, M. 1999, 'Ambient noise imaging in warm shallow seas; second-order moment and model-based imaging algorithms', *J. Acoust. Soc. Am.*, vol. 106, no. 6, pp. 3201-3210.

Vastola, K.S. 1984, 'Threshold detection in narrow-band non-Gaussian noise', *IEEE Trans. Commun.*, vol. COM-32, no. 2, pp. 134-139.

Versluis, M. Schmitz, B. von der Heydt, A. & Lohse, D. 2000, 'How snapping shrimp snap: through cavitation bubbles', *Science,* vol. 289, pp. 2114-2117.